ACS APPLIED MATERIALS & INTERFACES

Research Article

www.acsami.org

# Transfer Printing of Thermoreversible Ion Gels for Flexible Electronics

Keun Hyung Lee,[†] Sipei Zhang,[†] Yuanyan Gu,[‡] Timothy P. Lodge,[†,‡,*] and C. Daniel Frisbie[†,*]

[†]Department of Chemical Engineering and Materials Science, University of Minnesota, 421 Washington Avenue SE, Minneapolis, Minnesota 55455, United States

[‡]Department of Chemistry, University of Minnesota, 207 Pleasant Street SE, Minneapolis, Minnesota 55455, United States

Supporting Information

**ABSTRACT:** Thermally assisted transfer printing was employed to pattern thin films of high capacitance ion gels on polyimide, poly(ethylene terephthalate), and $SiO_2$ substrates. The ion gels consisted of 20 wt % block copolymer poly(styrene-*b*-ethylene oxide-*b*-styrene and 80 wt % ionic liquid 1-ethyl-3-methylimidazolium bis(trifluoromethyl sulfonyl)amide. Patterning resolution was on the order of 10 $\mu$m. Importantly, ion gels containing the block polymer with short PS end blocks (3.4 kg/mol) could be transfer-printed because of thermoreversible gelation that enabled intimate gel–substrate contact at 100 °C, while gels with long PS blocks (11 kg/mol) were not printable at the same temperature due to poor wetting contact between the gel and substrates. By using printed ion gels as high-capacitance gate insulators, electrolyte-gated thin-film transistors were fabricated that operated at low voltages (<1 V) with high on/off current ratios (~$10^5$). Statistical analysis of carrier mobility, turn-on voltage, and on/off ratio for an array of printed transistors demonstrated the excellent reproducibility of the printing technique. The results show that transfer printing is an attractive route to pattern high-capacitance ion gels for flexible thin-film devices.

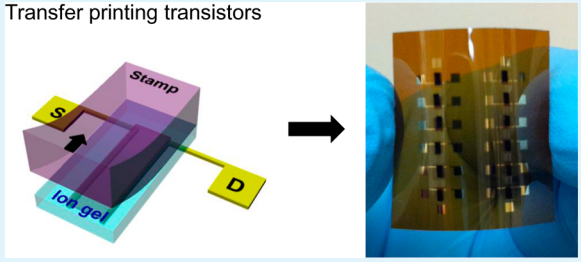


**KEYWORDS:** *transfer printing, thin-film transistor, polymer electrolyte, ion gel, ionic liquid*

## 1. INTRODUCTION

Gel electrolytes, also known as ion gels, have recently emerged as promising high-capacitance electronic insulator materials for printed-circuit applications.[1−6] The high capacitance is derived from mobile ions within the gels that, upon application of an external electric field, either (1) form electrical double layers (EDLs) at gel/semiconductor or gel/metal interfaces, or (2) supply necessary counterions for electrochemical oxidation or reduction processes at these interfaces. Importantly, while ion gels are ionically conducting, they are electronically insulating over a voltage window prescribed by the electrochemical stability of the component ions. Thus, ion gels may serve as high-capacitance insulators in thin-film devices such as capacitors, low-voltage thin-film transistors (TFTs), and biosensors.[6−8]

Ion gels can be formed using various chemistries, but an effective approach is to combine a room-temperature ionic liquid with a physically cross-linked block polymer.[9,10] Physical crosslinking is a versatile route, because the gel structures and properties can be controlled by changing the polymer block lengths, identities, and sequence.[11] For example, an ABA triblock copolymer with an ionic liquid soluble B middle block and insoluble A end blocks can form a soft gel by blending a few weight percent of the polymer in ionic liquids.[10] The low weight fraction of block polymer keeps the ionic conductivity of the composite high. Moreover, ABA gels with short A end-blocks can melt or further soften at high temperatures,[12,13] which is advantageous in material processing, as we will demonstrate here, because it allows coating or lamination processes in the viscous state with reversible solidification and stiffening on cooling.

Incorporation of ion gels into electronic devices requires methods to pattern thin films of these materials. Previously, both spin coating and aerosol jet printing have been successfully utilized to incorporate ion gels in TFTs.[1−3,14−16] However, alternative deposition strategies are desirable for high throughput and to provide a diversity of processing options. Transfer printing is an attractive option, as it has been employed to pattern films of organic small molecules, polymers, and quantum dots.[17−30] In this method, an elastomeric stamp (e.g., poly(dimethylsiloxane), PDMS) is employed to transfer a target layer to a receiving substrate (additive mode), or to remove a functional layer from a substrate by contact with a stamp (subtractive mode). In the additive mode, quantitative transfer of a target layer from the rubber stamp to a receiving substrate is determined by the difference of adhesion force for each layer.[31] To transfer an ink layer, the attractive interaction between the ink and the substrate should be larger than that of the ink/stamp interface.[31]

**Received:** June 17, 2013
**Accepted:** September 12, 2013
**Published:** September 12, 2013

 © 2013 American Chemical Society  dx.doi.org/10.1021/am402200n | *ACS Appl. Mater. Interfaces* 2013, 5, 9522−9527

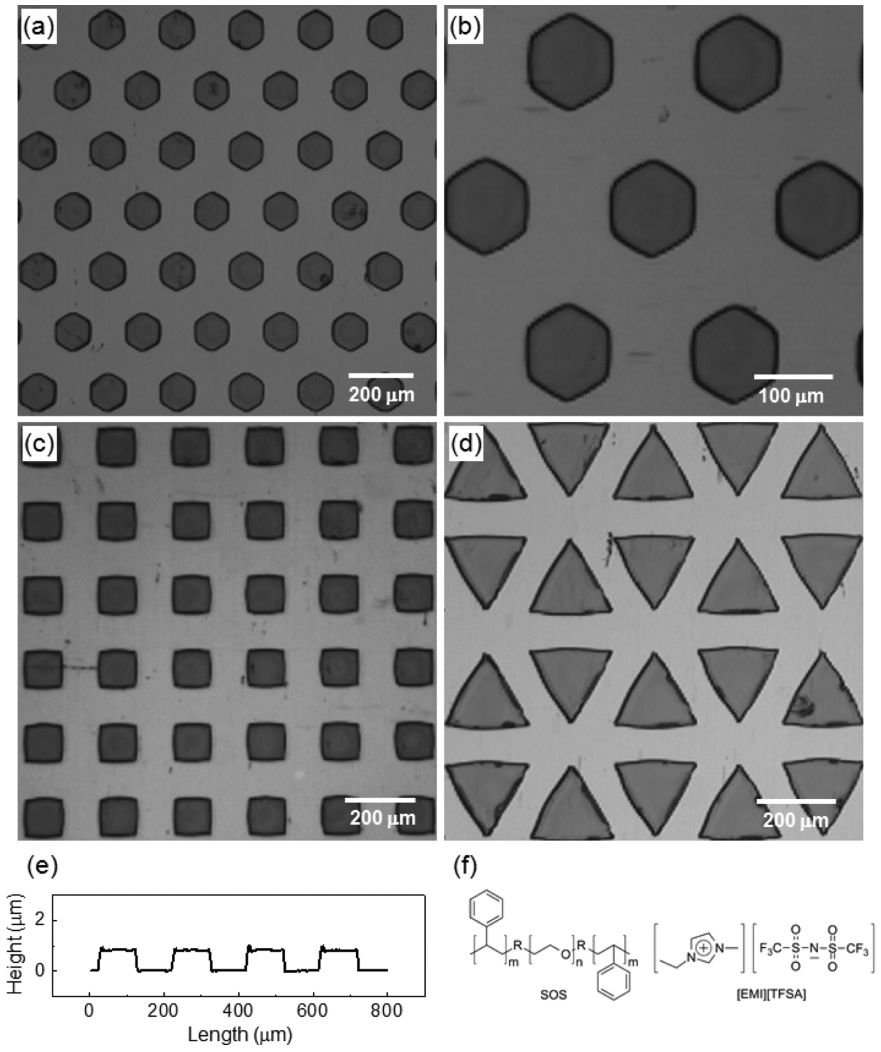


**Figure 1.** Optical microscope images of a patterned ion gel array on polyimide: (a, b) hexagons, (c) squares, and (d) triangles. (e) Height profile of the patterned squares in panel (c); the thickness of the squares was 0.8 $\mu$m. (f) Chemical structures of SOS and [EMI][TFSA]. The weight ratio of block polymer to ionic liquid was 1:4.

In this paper, we investigate the transfer-printing of ion gels on various substrates using patterned rubber stamps. The ion gel comprises a structuring polymer, poly(styrene-*b*-ethylene oxide-*b*-styrene) SOS, and a room-temperature ionic liquid, 1-ethyl-3-methylimidazolium bis(trifluoromethyl sulfonyl)amide, [EMI][TFSA]. The patches of printed ion gel have lateral dimensions of tens of micrometers, with thicknesses in the range of 0.5−2 $\mu$m. To demonstrate that these transfer-printed ion gel films can exhibit their intended electronic function, we have also fabricated electrolyte-gated thin-film transistors (EGTs)[32] by transfer-printing all active device layers (semiconductor, ion gel, and gate electrode) onto substrates with pre-patterned Au source/drain electrodes. The transfer-printed EGTs exhibit high transistor-output current (> 1 mA) at low operating voltages (< 1 V), as expected. We have also investigated the mechanism of the ion gel transfer printing process. Importantly, an SOS ion gel ($IG_{s\text{-}PS}$) with short PS end-blocks is transfer-printable, whereas SOS gels ($IG_{l\text{-}PS}$) with the long PS end-blocks are not; this difference is attributable to the thermoreversible gelation of copolymers with short PS blocks, which enables the rapid formation of intimate gel-substrate contact simply by heating the gel to temperatures above the gelation point.

## 2. RESULTS AND DISCUSSION

To transfer print an ion gel from a PDMS stamp to the receiving substrate by an additive mode, the $IG_{s\text{-}PS}$ gel was first directly spin-coated on a patterned PDMS stamp. The spin-coating solution was prepared by co-dissolving block polymer and [EMI][TFSA] in ethyl acetate. The inked stamp was manually placed on a receiving substrate. The assembly was then heated at 100 °C, above the gelation temperature ($T_{gel}$) of the ion gel, for 10 s to facilitate the development of intimate interfacial contact between the rough ion gel and substrate. Ion-gel transfer was achieved by slowly detaching the stamp from the substrate after cooling the assembly for a few seconds at room temperature. This process could be repeated multiple times with the same stamp. The physical origins of the printing process will be discussed later.

Figure 1 displays arrays of $IG_{s\text{-}PS}$ ion gels with three different shapes (hexagons, squares, and triangles) created on a polyimide substrate by transfer printing. For hexagons, the sides are ∼60 $\mu$m, and inter-pattern spacing between hexagons is ∼100 $\mu$m. Each square has side length of ∼100 $\mu$m, and the spacing is ∼100 $\mu$m. Triangles have ∼200 $\mu$m sides and pattern spacing of ∼50 $\mu$m. Clean edges and corners of the patterned


dx.doi.org/10.1021/am402200n | ACS Appl. Mater. Interfaces 2013, 5, 9522−9527

ion gels confirm that the transfer printing by PDMS stamps is reliable for a variety of polygons with acute, right, and obtuse angles. Figure 1e shows a height profile of the printed ion gels obtained with a surface profiler. The chemical structures of SOS and [EMI][TFSA] are shown in Figure 1f. Ion gels with two different thicknesses (~0.8 $\mu$m and ~1.5 $\mu$m) were obtained by changing the inking solution concentration, as shown in the Supporting Information (Figure S1). We have also successfully printed ion gels on poly(ethylene terephthalate) (PET) and $SiO_2$ substrates, and the results are also displayed in the Supporting Information (Figure S2).

To study the inherent electrical properties of an ion gel, ionic conductivity and capacitance measurements were conducted on an almost identical ion gel system consisting of 10 wt % SOS(3-35-3) and 90 wt % [EMI][TFSA], and the results are shown in the Supporting Information (Figure S3). (The numbers in parentheses are the number average molecular weights of each polymer block in kg/mol.) Measured ionic conductivity and capacitance values are consistent with those of other ion gels and pure ionic liquid reported previously.[10,13,33−36] As expected, ionic conductivity values are slightly lower than those of pure [EMI][TFSA] due to the obstruction by non-conductive polystyrene cores.[10,13] Very high capacitance values (>1 $\mu$F/cm$^2$) obtained over the investigated temperature range imply the formation of the electrical double layers.[16]

By transfer-printing $IG_{s\text{-}PS}$ as a high-capacitance gate insulator, we have fabricated EGTs. The other two polymer layers (semiconductor and gate electrode) were also separately patterned using the same method. An EGT was created by sequentially transfer-printing in three steps the semiconductor regioregular poly(3-hexylthiophene) (P3HT),[37] $IG_{s\text{-}PS}$, and a poly(3,4-ethylene dioxythiophene):poly(styrene sulfonate) (PEDOT:PSS) gate electrode[22] on a source/drain channel in a bottom-contact configuration. To deposit polymeric inks on a PDMS stamp, solution-casting methods were used. P3HT and the gel were spin-coated on a flat PDMS stamp, whereas the PEDOT:PSS gate electrode was deposited by drop casting. The inked stamp was manually cut to the desired size using a razor blade and then placed on a source/drain channel. The assembly was then heated at elevated temperature (80 °C for P3HT and PEDOT:PSS and 100 °C for the ion gel) to facilitate adhesion between the ink/substrate interfaces. Functional-layer transfer occurred upon detaching the stamp from the substrate at room temperature.

A cross-sectional schematic and an optical image of one transfer-printed EGT are shown in Figure 2a. The channel length ($L$) and width ($W$) of the devices are 100 $\mu$m and 1 mm, respectively. Figure 2b displays an optical image of an array of transfer-printed EGTs on a flexible polyimide substrate. It is noteworthy that all active layers (the semiconductor, the gate insulator, and the gate electrode) of the transistor were prepared by the simple lamination and detachment processes. These processes should also be compatible with roll-to-roll (R2R) fabrication.

Figure 2c shows the quasi-static output characteristics ($I_D$−$V_D$, where $I_D$ is the drain current and $V_D$ is the drain voltage) of a transfer-printed EGT at five different gate voltage ($V_G$) values. The output characteristics exhibited an increase in channel current with increasing (negative) $V_G$, i.e., $p$-channel behavior. A saturation current above 2 mA was obtained at $V_G$ = −1 V and $V_D$ = −1 V. Low-voltage transistor operation can be attributed to the large capacitance of the ion gel, which is ~10

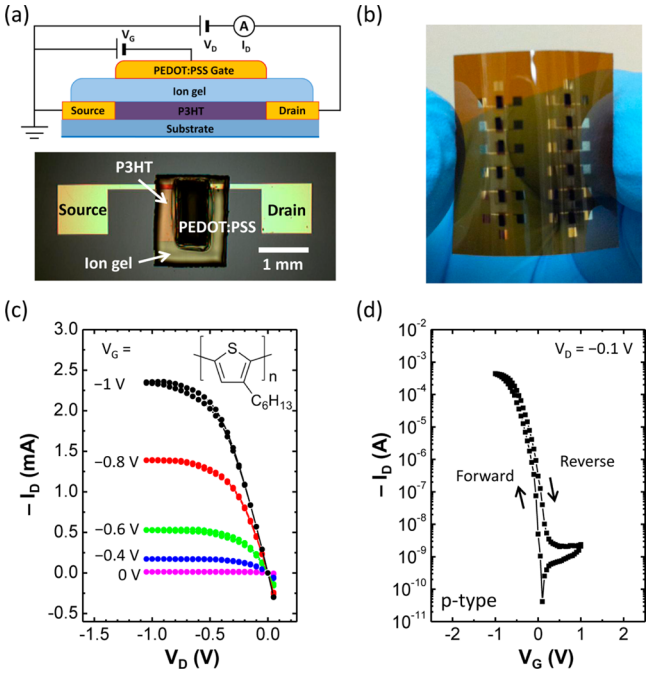


**Figure 2.** (a) Cross-sectional schematic of an electrolyte-gated thin-film transistor (EGT) (top) and an optical image of an EGT on $SiO_2$ (bottom). The device has channel length of 100 $\mu$m and width of 1 mm. (b) Optical image of an all-printed transistor array fabricated on a flexible polyimide substrate. (c) Quasi-static $I_D$−$V_D$ characteristics of an EGT. Inset shows the chemical structure of P3HT. (d) Quasi-static $I_D$−$V_G$ characteristic of an EGT. The gate voltage was swept at a rate of 5 mV/s.

$\mu$F/cm$^2$.[15] The accumulated hole density in the P3HT film will be discussed shortly.

Figure 2d shows the quasi-static transfer characteristic ($I_D$−$V_G$) of the $p$-channel EGT (see the Supporting Information (Figure S4) for the corresponding $I_G$−$V_G$ plot, where $I_G$ is the gate-source current). Drain current was measured while sweeping $V_G$ from 1 V to −1 V and then back to 1 V at a rate of 5 mV/s at a constant $V_D$ value of −0.1 V. A small $V_D$ value was applied to ensure the device operated in the linear regime. The device displayed a reasonable on/off current ratio (>10$^5$). The hole mobility ($\mu$) of the transistors was calculated in the linear regime using the following equation (eq 1):

$$\mu = \frac{L}{W}\left(\frac{I_D}{epV_D}\right) \quad (1)$$

where $e$ is the elementary charge and $p$ is the induced hole density in P3HT. The value of $p$ was obtained by dynamic gate-displacement current ($I_{disp}$) measurements (see the Supporting Information (Figure S5)). In the measurement, the source and drain contacts were connected to ground while the gate potential was swept at different rates. By plotting $\int I_{disp}dV_G/(r_V eA)$ versus $1/r_V$, where $r_V$ is the gate potential sweep rate and $A$ is the area of the ion gel, the hole density ($p$) accumulated in the semiconductor channel can be extracted from the $y$-intercept.[38,39] A high hole density of 1.2 × 10$^{15}$ cm$^{-2}$ was thus obtained. This is attributable to electrochemical doping in the P3HT film, which results in three-dimensional (3D) carrier accumulation.[40] In this case, a 3D hole density, which we estimate to be 2.4 × 10$^{20}$ cm$^{-3}$ from the thickness of the P3HT film, is a more appropriate metric. The room-temperature

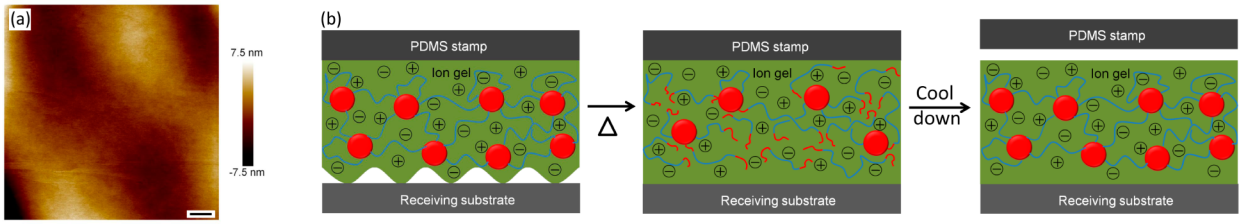


**Figure 3.** (a) An AFM height image of an $IG_{s\text{-}PS}$ (scale bar = 5 $\mu$m) film, indicating nanometer-scale roughness. (b) Schematic of ion-gel transfer from a PDMS stamp to a receiving substrate. Initial contact is made between ion gel-coated PDMS and a substrate (left). An ion gel with short PS end-blocks achieves intimate contact with a receiving substrate upon heating above $T_{gel}$ (middle). The ion gel is transferred upon detaching PDMS (right).

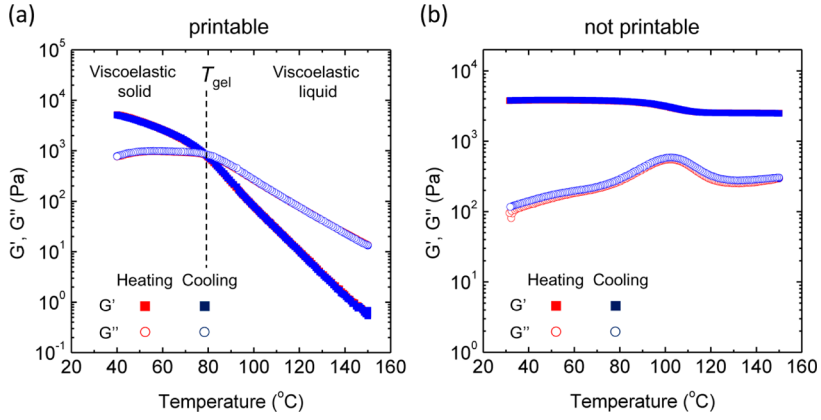


**Figure 4.** Temperature-dependent dynamic shear moduli ($G'$ and $G''$) for (a) $IG_{s\text{-}PS}$ (10 wt % SOS(3.4-35-3.4) in [EMI][TFSA]) and (b) $IG_{l\text{-}PS}$ (10 wt % SOS(11-35-11) in [EMI][TFSA]) at a frequency $\omega$ = 0.3 rad/s and strain $\gamma$ = 5% (for a) or 1% (for b) with heating and cooling rates of ±1 °C/min.

mobility for P3HT gated with the transfer-printed ion gel was 1.5 $cm^2/(V\ s)$, which is comparable to that of P3HT EGTs prepared by aerosol jet printing.[1,2] This mobility is an order of magnitude larger than that of P3HT gated with conventional dielectrics,[41,42] presumably because of the extremely large number of holes induced by the ion gel that fill the carrier traps in the P3HT film. Some $I_D$ hysteresis is observed between forward and reverse sweeps, which is likely due to the large thickness of the transfer-printed ion gel film.[43]

We have also fabricated EGTs using another thermoresponsive ion gel based on the pentablock polymer poly(*N*-isopropyl acrylamide-*b*-styrene-*b*-ethylene oxide-*b*-styrene-*b*-*N*-isopropyl acrylamide) (NSOSN) and [EMI][TFSA].[12] The NSOSN ion gel was transfer-printed at a lower temperature of 70 °C (versus 100 °C for SOS gels), because of the low $T_{gel}$ of ~50 °C. This demonstrates that the process temperature can be controlled by simply tailoring the block-polymer architecture. $I_D-V_G$ curves for 35 transistors using an NSOSN gel as the gate insulator are displayed in the Supporting Information (Figure S6). The transistors behaved nearly identically, with an average hole mobility of 1.5 ± 0.5 $cm^2/(V\ s)$ and on/off current ratio of 4.3 (± 3.2) × $10^5$. The turn-on voltage, where the drain current in the forward sweep passes the off current of the reverse sweep, remained near 0 V for all transistors. These results indicate that transfer printing provides a reliable alternative for processing functional ion gels with high reproducibility.

The physical basis of ion-gel transfer can be explained by the relative adhesion between two interfaces, i.e., PDMS/ion gel and the ion gel/receiving substrate.[31] When the ion gel preferentially sticks to the receiving substrate rather than to a PDMS surface, it can be transferred from PDMS to the receiving substrate as a result of adhesive failure at the PDMS surface. Since the ion gel is composed mostly of ionic liquid (more than 80 wt %), printability of the ion gel can be estimated by the contact angles of the ionic liquid on donor and acceptor films. The measured contact angles of [EMI][TFSA] on PDMS, polyimide, $SiO_2$, PET, and P3HT are 80° ± 2°, 12° ± 2°, 37° ± 1°, 65° ± 3°, and 54° ± 1°, respectively (see the Supporting Information (Figure S7)). This result indicates that [EMI][TFSA] wets the receiving substrates (polyimide, $SiO_2$, PET, and P3HT) better than the PDMS surface, which facilitates ion gel transfer from PDMS to the target substrates. However, in addition to preferential wetting, the ion gel must form intimate contact with the substrate to maximize gel/receiving substrate adhesion for successful transfer. In this regard, it is important that $IG_{s\text{-}PS}$ is printable only after annealing the sample at temperatures above $T_{gel}$.

Figure 3 illustrates how the ion gel/substrate interface determines the printability for $IG_{s\text{-}PS}$. When the ion gel-coated stamp is placed on a substrate, the ion gel does not achieve intimate contact with the substrate, primarily because of the rough nature of ion gels. For example, the $IG_{s\text{-}PS}$ surface exhibits bumps with peak-to-valley heights of ~10 nm (Figure 3a). At temperatures above $T_{gel}$, the PS blocks can pull out from the cores of the micelles and the $IG_{s\text{-}PS}$ gel becomes more fluidlike. The melted solution then wets the substrate and achieves intimate physical contact (Figure 3b, middle). Upon cooling below $T_{gel}$, the gel reforms and the applied external tensile force then causes adhesive failure at the PDMS interface, because the ion gel prefers to stick on the recipient surfaces (Figure 3b, right). In contrast, $IG_{l\text{-}PS}$ cannot achieve conformal contact with substrates, even at elevated temperatures, because the gel


dx.doi.org/10.1021/am402200n | ACS Appl. Mater. Interfaces 2013, 5, 9522−9527

remains too solidlike. This is due to the high enthalpic barrier for pulling longer PS chains out from the network cores, which results in failure of ion gel transfer.

The temperature-dependent viscoelastic properties of the ion gels highlight the crucial role of the PS block length in the printing process. Figure 4a shows the sol−gel transition of $IG_{s\text{-}PS}$ with 10 wt % of SOS(3.4-35-3.4) in [EMI][TFSA] upon varying the temperature between 40 °C and 150 °C, with heating and cooling rates of ±1 °C/min. At low temperature, the values of the dynamic moduli $G'$ and $G''$ are high, and $G' > G''$, indicating solidlike behavior. With increasing temperature, both $G'$ and $G''$ decrease, and $G''$ is greater than $G'$, indicating a liquidlike state. The crossover of $G'$ and $G''$, or $T_{gel}$, is ∼80 °C for the $IG_{s\text{-}PS}$ used in this study. Therefore, at $T > T_{gel}$, PS chains in $IG_{s\text{-}SP}$ can be readily pulled out from the micellar cores and the gel can intimately wet the recipient material, which is a critical step for the gel transfer.

Note that $IG_{s\text{-}PS}$ with 20 wt % SOS(3.4-35-3.4) in [EMI][TFSA] is also transferrable, although the system remains an elastic solid ($G' > G''$) with two plateaus over the entire temperature range (see the Supporting Information (Figure S8a)); i.e., fully liquid-like behavior above $T_{gel}$ is not necessary for transfer printing. As in the 10 wt % case, at low temperatures $G'$ shows a rubbery plateau typical of a physically cross-linked network, because of the high enthalpic barrier for PS chain pullout from the micellar cores. At high temperature, however, PS chains can diffuse out from the crosslinks, as noted above. When the polymer concentration is higher (e.g., 20 wt %), a congested micelle solution consisting of insoluble PS cores and PEO coronas is formed.[12,13] This congested solution behaves as a viscoelastic solid with a lower modulus. Our previous study on SOS(3-35-3) ion gels reveals that the PS chain pull out rate from the network cores does not depend strongly on the polymer concentration for this type of thermoresponsive ion gel.[12,13] PS chain pull out does occur at $T > T_{gel}$, and thus the viscoelastic gel can flow and wet the substrate.

On the other hand, $IG_{l\text{-}PS}$ with SOS (11-35-11) shows characteristic features of a cross-linked network over the entire temperature range, $G' > G''$ (see Figure 4b and Figure S8b in the Supporting Information). This implies that PS chains in $IG_{l\text{-}PS}$ cannot be pulled out from the cores, which results in poor contact between rough $IG_{l\text{-}PS}$ film and the substrate because viscoelastic flow is impeded. (Note that the relaxation observed at ∼100 °C in Figure 4b and Figure S8b in the Supporting Information corresponds to the glass transition of the PS chains, not pullout.) This observation is consistent with the unsuccessful patterning for $IG_{l\text{-}PS}$ shown in the Supporting Information (Figure S9).

## 3. CONCLUSIONS

We have successfully transfer-printed hexagonal, square, and triangular poly(styrene-*b*-ethylene oxide-*b*-styrene) (SOS) ion gels with short PS end-blocks ($IG_{s\text{-}PS}$) on three different substrates with two different thicknesses. Interestingly, $IG_{s\text{-}PS}$ is transfer-printable because of its ability to form intimate wetting contact with the receiving substrate, while SOS ion gels with long PS end-blocks ($IG_{l\text{-}PS}$) are not due to the high enthalpic barrier keeping the PS chains locked in PS micellar cores. Contact angle measurements of 1-ethyl-3-methylimidazolium bis(trifluoromethyl sulfonyl)amide ([EMI][TFSA]) on a donor poly(dimethylsiloxane) (PDMS) substrate and recipient polyimide, PET, $SiO_2$, and P3HT surfaces suggest that the ion gel wets the receiving substrates better than the PDMS. We have fabricated electrolyte-gated thin-film transistors (EGTs) using transfer-printed ion gels as high-capacitance gate insulators on $SiO_2$ and flexible polyimide substrates. All printed EGTs operated at very low voltages (<1 V) and displayed high on/off current ratios (∼$10^5$). Device statistics for carrier mobility, turn-on voltage, and on/off ratio exhibited the excellent reproducibility of the printing technique. Overall, these results demonstrate that transfer printing provides an attractive option to pattern thermoreversible ion gel electrolyte layers for use in flexible electronic devices.

## ■ ASSOCIATED CONTENT

### Supporting Information

Experimental procedures, transfer-printed ion gels with different thicknesses, ion gels on various substrates, impedance results, $I_G-V_G$ and $I_{disp}-V_G$ characteristics, transistor statistics, contact angle measurements, temperature-dependent dynamic shear moduli measurements, and unsuccessful pattering result. This material is available free of charge via the Internet at http://pubs.acs.org.

## ■ AUTHOR INFORMATION

### Corresponding Author

*E-mail: lodge@umn.edu (T.P.L), frisbie@umn.edu (C.D.F).

### Notes

The authors declare no competing financial interest.

## ■ ACKNOWLEDGMENTS

The authors thank Dr. Yiyong He for providing the NSOSN block copolymer, Yanfei Wu for AFM measurements, and Chang Hyun Kim for helpful discussions. This work is supported by the Air Force Office of Scientific Research (Award No. FA9550-12-1-0067) and the MRSEC Program of the National Science Foundation (under Award No. DMR-0819885). Partial support was also provided by the Abu Dhabi Minnesota Institute for Research Excellence (ADMIRE), which is a partnership between the Petroleum Institute of Abu Dhabi and the Department of Chemical Engineering and Materials Science of the University of Minnesota.

## ■ REFERENCES

(1) Cho, J. H.; Lee, J.; Xia, Y.; Kim, B.; He, Y.; Renn, M. J.; Lodge, T. P.; Frisbie, C.D. *Nat. Mater.* **2008**, *7*, 900−906.
(2) Xia, Y.; Zhang, W.; Ha, M.; Cho, J. H.; Renn, M. J.; Kim, C. H.; Frisbie, C. D. *Adv. Funct. Mater.* **2010**, *20*, 587−594.
(3) Ha, M.; Xia, Y.; Green, A. A.; Zhang, W.; Renn, M. J.; Kim, C. H.; Hersam, M. C.; Frisbie, C. D. *ACS Nano* **2010**, *4*, 4388−4395.
(4) Lee, S.-K.; Kim, B. J.; Jang, H.; Yoon, S. C.; Lee, C.; Hong, B. H.; Rogers, J. A.; Cho, J. H.; Ahn, J.-H. *Nano Lett.* **2011**, *11*, 4642−4646.
(5) Chen, P.; Fu, Y.; Aminirad, R.; Wang, C.; Zhang, J.; Wang, K.; Galatsis, K.; Zhou, C. *Nano Lett.* **2011**, *11*, 5301−5308.
(6) Kim, S. H.; Hong, K.; Xie, W.; Lee, K. H.; Zhang, S.; Lodge, T. P.; Frisbie, C. D. *Adv. Mater.* **2013**, *25* (13), 1822−1846 (DOI: 10.1002/adma.201202790).
(7) Berggren, M.; Richter-Dahlfors, A. *Adv. Mater.* **2007**, *19*, 3201−3213.
(8) Mabeck, J. T.; Malliaras, G. G. *Anal. Bioanal. Chem.* **2006**, *384*, 343−353.
(9) Susan, M. A. B. H.; Kaneko, T.; Noda, A.; Watanabe, M. *J. Am. Chem. Soc.* **2005**, *127*, 4976−4983.
(10) He, Y.; Boswell, P. G.; Buhlmann, P.; Lodge, T. P. *J. Phys. Chem. B* **2007**, *111*, 4645−4652.
(11) Lodge, T. P. *Science* **2008**, *321*, 50−51.

(12) He, Y.; Lodge, T. P. *Macromolecules* **2008**, *41*, 167−174.
(13) Zhang, S.; Lee, K. H.; Sun, J.; Frisbie, C. D.; Lodge, T. P. *Macromolecules* **2011**, *44*, 8981−8989.
(14) Yomogida, Y.; Pu, J.; Shimotani, H.; Ono, S.; Hotta, S.; Iwasa, Y.; Takenobu, T. *Adv. Mater. 24*, 4392−4397.
(15) Lee, K. H.; Kang, M. S.; Zhang, S.; Gu, Y.; Lodge, T. P.; Frisbie, C. D. *Adv. Mater.* **2012**, *24*, 4457−4462.
(16) Lee, K. H.; Zhang, S.; Lodge, T. P.; Frisbie, C. D. *J. Phys. Chem. B* **2011**, *115*, 3315−3321.
(17) Menard, E.; Meitl, M. A.; Sun, Y.; Park, J.-U.; Shir, D. J.-L.; Nam, Y.-S.; Jeon, S.; Rogers, J. A. *Chem. Rev.* **2007**, *107*, 1117−1160.
(18) Xia, Y.; Whitesides, G. M. *Angew. Chem., Int. Ed. Engl.* **1998**, *37*, 550−575.
(19) Xia, Y.; Whitesides, G. M. *Annu. Rev. Mater. Sci.* **1998**, *28*, 153−184.
(20) Suh, D.; Choi, S. J.; Lee, H. H. *Adv. Mater.* **2005**, *17*, 1554−1560.
(21) Meitl, M. A.; Zhu, Z.-T.; Kumar, V.; Lee, K. J.; Feng, X.; Huang, Y. Y.; Adesida, I.; Nuzzo, R. G.; Rogers, J. A. *Nat. Mater.* **2006**, *5*, 33−38.
(22) Granlund, T.; Nyberg, T.; Stolz Roman, L.; Svensson, M.; Inganäs, O. *Adv. Mater.* **2000**, *12*, 269−273.
(23) Lee, T.-W.; Zaumseil, J.; Bao, Z.; Hsu, J. W. P.; Rogers, J. A. *Proc. Natl. Acad. Sci. U.S.A.* **2004**, *101*, 429−433.
(24) Li, D.; Guo, L. J. *Appl. Phys. Lett.* **2006**, *88*, 063513-1−063513-3.
(25) Cosseddu, P.; Bonfiglio, A. *Appl. Phys. Lett.* **2006**, *88*, 023506-1−023506-3.
(26) Emah, J. B.; Curry, R. J.; Silva, S. R. P. *Appl. Phys. Lett.* **2008**, *93*, 103301-1−103301-3.
(27) Chen, L.; Degenaar, P.; Bradley, D. D. C. *Adv. Mater.* **2008**, *20*, 1679−1683.
(28) Serban, D. A.; Greco, P.; Melinte, S.; Vlad, A.; Dutu, C. A.; Zacchini, S.; Iapalucci, M. C.; Biscarini, F.; Cavallini, M. *Small* **2009**, *5*, 1117−1122.
(29) Kim, T.-H.; Cho, K.-S.; Lee, E. K.; Lee, S. J.; Chae, J.; Kim, J. W.; Kim, D. H.; Kwon, J.-Y.; Amaratunga, G.; Lee, S. Y.; Choi, B. L.; Kuk, Y.; Kim, J. M.; Kim, K. *Nat. Photon.* **2011**, *5*, 176−182.
(30) Kang, S. J.; Kim, B.; Kim, K. S.; Zhao, Y.; Chen, Z.; Lee, G. H.; Hone, J.; Kim, P.; Nuckolls, C. *Adv. Mater.* **2011**, *23*, 3531−3535.
(31) Park, S. Y.; Kwon, T.; Lee, H. H. *Adv. Mater.* **2006**, *18*, 1861−1864.
(32) Lee, J.; Panzer, M. J.; He, Y.; Lodge, T. P.; Frisbie, C. D. *J. Am. Chem. Soc.* **2007**, *129*, 4532−4533.
(33) Zhang, S.; Lee, K. H.; Frisbie, C. D.; Lodge, T. P. *Macromolecules* **2011**, *44*, 940−949.
(34) Tokuda, H.; Hayamizu, K.; Ishii, K.; Susan, M. A. B. H.; Watanabe, M. *J. Phys. Chem. B* **2005**, *109*, 6103−6110.
(35) Drüschler, M.; Huber, B.; Passerini, S.; Roling, B. *J. Phys. Chem. C* **2010**, *114*, 3614−3617.
(36) Alam, M. T.; Islam, M. M.; Okajima, T.; Ohsaka, T. *J. Phys. Chem. C* **2008**, *112*, 16600−16608.
(37) Kim, H.; Yoon, B.; Sung, J.; Choi, D.-G.; Park, C. *J. Mater. Chem.* **2008**, *18*, 3489−3495.
(38) Liang, Y.; Frisbie, C. D.; Chang, H.-C.; Ruden, P. P. *J. Appl. Phys.* **2009**, *105*, 024514−024516.
(39) Xie, W.; Frisbie, C. D. *J. Phys. Chem. C* **2011**, *115*, 14360−14368.
(40) Lee, J.; Kaake, L. G.; Cho, J. H.; Zhu, X. Y.; Lodge, T. P.; Frisbie, C. D. *J. Phys. Chem. C* **2009**, *113*, 8972−8981.
(41) Bao, Z.; Dodabalapur, A.; Lovinger, A. J. *Appl. Phys. Lett.* **1996**, *69*, 4108−4110.
(42) Sirringhaus, H.; Brown, P. J.; Friend, R. H.; Nielsen, M. M.; Bechgaard, K.; Langeveld-Voss, B. M. W.; Spiering, A. J. H.; Janssen, R. A. J.; Meijer, E. W.; Herwig, P.; de Leeuw, D. M. *Nature* **1999**, *401*, 685−688.
(43) Cho, J. H.; Lee, J.; He, Y.; Kim, B. S.; Lodge, T. P.; Frisbie, C. D. *Adv. Mater.* **2008**, *20*, 686−690.